

## Rearrangements in hard-sphere glasses under oscillatory shear strain

G. Petekidis,\* A. Moussaïd, and P. N. Pusey

*Department of Physics and Astronomy, The University of Edinburgh, Mayfield Road, Edinburgh, EH9 3JZ, United Kingdom*

(Received 21 April 2002; published 26 November 2002)

We investigate particle rearrangements in colloidal glasses subjected to oscillatory shear strain by the technique of light scattering (LS) echo. LS echo directly follows the motion of the particles through peaks (echoes) in the intensity autocorrelation function; the height of the peak measures the reversible motion in the sample. Polydisperse hard-sphere poly-methylmethacrylate particles were used to avoid crystallization under shear. The yielding behavior is monitored through irreversible particle rearrangements at several volume fractions in the glass phase region. At high volume fractions the glasses are found to yield at strains as high as 15% while the irreversible rearrangements have a more gradual onset with strain for low volume fraction glasses. The behavior of high order echoes at long times is related to the effects of shear on the frozen-in fluctuations of the glass.

DOI: 10.1103/PhysRevE.66.051402

PACS number(s): 82.70.Dd, 81.40.-z, 83.50.-v

### I. INTRODUCTION

A common characteristic of a number of soft materials is that at high enough concentrations they behave as weak amorphous solids. When subjected to shear strain they respond elastically at low stress (or strains) and plastically at high ones. In concentrated particle suspensions shear strain may induce a disorder to order transition and yielding can then be related both to such a transition and to further structural changes of the crystalline sample.

Shear-induced crystallization of suspensions of hard-sphere colloids has been studied by light scattering [1–3] and has marked effects on the rheological behavior [4], leading to a decrease of the suspension's viscosity (shear thinning). However, shear thinning is not always accompanied by a flow-induced ordering [5,6] but is rather attributed more generally to a decrease of the Brownian contribution to the stress [7]. At higher shear rates, in concentrated systems, the viscosity increases (shear thickening) due to an increase of the hydrodynamic stress; the latter originates from the formation of nonpermanent, disordered clusters due to strong short-range lubrication forces [7]. Shear thinning and thickening of hard-sphere suspensions have been studied extensively by rheology [8–11] and simulations [6,7,13] while the microstructural changes in the shear thickening regime that have been predicted by theory and simulations [12,13] have been observed by small-angle neutron scattering [5,14].

In other systems such as concentrated emulsions, foams, or colloidal suspensions of polydisperse particles the sample retains its amorphous structure during the application of shear but also exhibits yielding with increasing strain (or stress) [15–17]. Theoretical models attribute such rheological similarities of soft materials to structural disorder and metastability and relate them to glass dynamics [18]. It has been argued that such disorder in concentrated dispersions creates energy barriers that cannot be overcome by thermal

fluctuations; application of stress, however, is expected to modify those energy landscapes so that different metastable states can be reached [18]. Other theoretical studies on driven mean-field disordered systems describe the behavior of a two-step relaxation with increasing driving force, suggesting that the slow glassy dynamics are speeded up with increasing drive, resulting in shear thinning, while aging is stopped [19]. Related to the above is the effect of shear (constant or oscillatory) on particle diffusion. Shear-induced diffusion in hard-sphere suspensions has been investigated experimentally [20,21] and theoretically [22] showing an anisotropic increase of the self-diffusion coefficient.

In general the dynamics of colloidal systems driven away from equilibrium by the application of shear flow are determined by the interplay of the intrinsic relaxation of the system with shear flow. Except at random close packing, small suspended particles move in thermally induced Brownian motion, thus rearranging themselves spontaneously even in the absence of shear. At low concentrations the particles move independently; at higher concentrations their motions become coupled through direct and hydrodynamic interactions. In highly concentrated suspensions particles are restricted in cages formed by neighboring particles, and thermal fluctuations evolve through a two-stage process:  $\beta$  relaxation, corresponding to a fast relatively free motion of particles in the cage (slowed by hydrodynamic interactions); and  $\alpha$  relaxation, an extremely slow diffusion at longer distances corresponding to cage breakdown [23,24]. In glasses the large-scale rearrangements which give rise to the slow mode are suppressed and the system becomes nonergodic. Shear, however, induces flow, which changes particle motion and can dramatically affect the dynamics of the system. A measure of the relative importance of Brownian and shear-induced motions is given by the Péclet number  $Pe = \dot{\gamma}\tau_B$  where  $\dot{\gamma}$  is the shear strain rate and  $\tau_B$  is the Brownian relaxation time [for a dilute system  $\tau_B = R^2/2D$ , where  $R$  is the particle radius and  $D (= k_B T/6\pi\eta R)$  is the Stokes-Einstein diffusivity of a noninteracting particle in a medium with viscosity  $\eta$ ]. For shear rates  $\dot{\gamma}$  much smaller than the Brownian relaxation rate  $1/\tau_B$  ( $\dot{\gamma}\tau_B \ll 1$ ) the intrinsic dynamics of the

---

\*Corresponding author. Present address: Institute of Electronic Structure and Laser—Foundation for Research and Technology, P. O. Box 1527, Vassilika Vouton, 71110, Heraklion, Crete, Greece.

system relax much faster than the rate at which shear disturbs the structure and thus no significant effect on the structure or the dynamics of the system is expected. If, however, the shear rate is sufficiently high ( $\dot{\gamma}\tau_B \geq 1$ ) so that the structure of the system is altered before it can relax back to equilibrium through its internal relaxation we may expect interesting effects on the structure and dynamics of the system.

Microdynamic information related to the particle trajectories in the sheared sample is essential to elucidate the mechanism of yield and shear-induced rearrangements. In this paper we present an experimental study of the response of glasses of polydisperse hard-sphere particles under oscillatory shear strain. The light scattering (LS) echo technique is used to follow the motion of the particles. In fact, we directly detect the reversibility of the motion of the particles undergoing periodic shear strain. Consequently the shear-induced irreversible rearrangements can be related to yielding of the colloidal glass. The progress of yielding with increasing strain amplitude is studied at several volume fractions in the glass regime. The paper is structured as follows. In Sec. II we present the technique of light scattering echo and in Sec. III the experimental aspects of the work related to (A) the samples and (B) the shear cell and the light scattering setup. The results are presented in Sec. IV and are discussed in Sec. V. Finally, the conclusions are presented in Sec. VI.

## II. LIGHT SCATTERING ECHO TECHNIQUE

In a dynamic light scattering (DLS) experiment the analysis of temporal fluctuations in scattered light provides information on the dynamics of the sample. Usually the time autocorrelation function of the scattered intensity,  $I(t)$ , of a single speckle, or diffraction spot, is measured. If the photons are scattered once (or not at all) in the sample—transparent, single-scattering sample—DLS detects a specific Fourier component of density fluctuations; thus the dynamics at a particular scattering wave vector,  $q [= (4\pi/\lambda)\sin\theta/2]$  with  $\lambda$  the wavelength in the medium and  $\theta$  the scattering angle] is determined [25]. If the photons are scattered many times—opaque sample—the technique is diffusing wave spectroscopy (DWS). In DWS the wave vector dependence is lost and the measured relaxation times depend on the scattering geometry (transmission or backscattering), rather than the actual scattering angle, as well as on the number of scattering events  $n$  (or the transport mean free path  $l^*$ ), the geometry of the incident beam, and the intrinsic dynamics of the sample [26–28].

A few years ago Hébraud *et al.* [16] and Höhler *et al.* [17] reported a clever development of DWS in which the sample is subjected to an oscillatory shear strain during the light scattering measurement. The motion of the scatterers induced by the shear strain causes the relative phases of the light scattered by the particles to change, so the speckle pattern changes. As the medium is distorted by the induced flow, fluctuations in the scattered light become decorrelated causing the measured normalized time autocorrelation function of the scattered intensity  $g^{(2)}(\tau) = \langle I(\tau+t)I(t) \rangle / \langle I(t) \rangle^2$  to decay. If, however, after one period  $T$  of oscillation (or an integral number of periods) the particles return exactly to

their original positions—a purely reversible deformation—then the speckle pattern also returns to its original configuration. The result is that  $g^{(2)}(\tau) - 1$  exhibits “echoes” of amplitude 1 at delay times equal to integral multiples of  $T$  (see Fig. 2 below). On the other hand, if shear induces some irreversible rearrangements and some of the particles do not return to their original positions, the echoes will have amplitudes smaller than 1; the reduction of the amplitude of the echoes provides a measure of the degree of the irreversible rearrangement. Thus this technique of DWS, or light scattering, echo can be used to investigate how soft matter yields and flows under the application of shear strain, in particular as a function of strain amplitude.

Hébraud *et al.* used the method to study the motion of droplets in disordered concentrated oil-in-water emulsions under oscillatory shear strain [16]. In the absence of any Brownian motion the emulsion droplets were found to rearrange irreversibly above a critical yield strain which increases with increasing concentration. As indicated by the drop of the echo amplitude, yielding occurred at relatively low strain amplitudes (below 8%). Furthermore, surprisingly, after the drop of the first echo the amplitudes of all the later echoes remain constant; such a behavior was attributed to localized yielding where, during the repetitive cycles of oscillatory shear, parts of the sample always strain elastically while other parts, completely disjoint from the former, strain always irreversibly. Hence, it is interesting to investigate whether such behavior is particularly characteristic of glasses of deformable droplets or is of a common origin in all particle glasses. DWS echo measurements in hard-sphere colloidal glasses were later presented by Haw *et al.* [29] in a study of shear-induced crystallization, but higher order echoes could not be measured due to limitations of the correlator used. The decay of the echoes observed was related to shear-induced ordering.

The aim of the work reported here is to investigate shear-induced phenomena in colloidal glasses. We use “hard-sphere” colloidal particles of poly-methylmethacrylate (PMMA). In order to avoid crystallization, the particles have a spread of size, or polydispersity, of about 12%. Thus we are able to study the microdynamic changes related to yield without the additional complication of a disorder to order transition. For this purpose we set up a precision oscillatory shear cell and develop and extend the DWS echo technique, originally applied [16] to samples in the limit of strong multiple scattering, to less turbid samples. The goal is to understand the microscopic rearrangements and the dynamics of such systems when driven far from equilibrium and their relations with macroscopic quantities such as yield strain.

The interpretation of the data obtained from our experiments is, for several reasons, quite complicated. Here we give a simplified theory which will allow a largely qualitative discussion of the results. For the simple case of a dilute suspension of particles undergoing Brownian motion and not strained, studied in the single-scattering regime (i.e., by ordinary DLS) we have [25]

$$\sqrt{g^{(2)}(\tau) - 1} = \exp\left(-\frac{1}{6}q^2\langle\Delta r^2(\tau)\rangle\right), \quad (1)$$

where  $\langle \Delta r^2(\tau) \rangle$  is the mean square displacement of a scatterer. In the strong multiple scattering limit it can be shown [28] that the correlation function in the transmission geometry can be approximated by

$$\sqrt{g^{(2)}(\tau)-1} \approx \exp\left(-\frac{1}{6}nk^2\langle \Delta r^2(\tau) \rangle\right), \quad (2)$$

where  $k=2\pi/\lambda$  ( $=q/2$  at  $\theta=180^\circ$ ). One consequence of Eq. (2) is immediately apparent: while ordinary DLS probes a length scale of order  $1/q$ , the length scale  $l_{DWS}$  probed by DWS,  $l_{DWS} \approx 1/\sqrt{nk}$ , is smaller by a factor equal to the square root of the number of scatterings. Thus, if we are interested in measuring particle displacements of order 100 nm or more, we cannot allow the number of scatterings  $n$  to be too large or  $\sqrt{g^{(2)}(\tau)-1}$  will decay to zero (or at least to the noise level) for displacements smaller than this. Thus, we are forced to work with a relatively small number of scatterings where Eq. (2), derived for the full DWS (strong scattering) limit, may not be valid. We note, however, that, although in the intermediate regime between single scattering and the DWS limit a quantitative description of dynamic light scattering is difficult, there is a rigorous theory for the case of double scattering [33]. According to this work the contribution of double scattering from a spherical scattering volume in the depolarized correlation function reads

$$\sqrt{g^{(2)}(\tau)-1} = \exp\left(-\frac{2}{3\alpha}k^2\langle \Delta r^2(\tau) \rangle\right), \quad (3)$$

where  $\alpha(kR, \theta)$  is a function of  $kR$  and of the scattering angle  $\theta$ . For  $2kR=5$  ( $R=180$  nm,  $\lambda=633$  nm) and  $\theta \approx 0$  we have  $\alpha \approx 2$ . Thus the dynamics measured under double-scattering conditions are the same as those predicted in the DWS approximation with  $n=2$ . In the work reported here, therefore, where we eliminate single scattering by using a polarizer (see below), we will assume that Eq. (3) [which coincides with Eq. (2) for  $n=2$  and  $\alpha \approx 2$ ] gives a reasonable (although approximate) description of the measured correlation function [30].

Equations (1)–(3) hold for noninteracting scatterers (dilute systems) and relate the measured quantity  $g^{(2)}(\tau)$  to the average microscopic motion of the particles in the sample. However, in concentrated suspensions, direct and hydrodynamic interactions between particles strongly affect their dynamics [31,32]. In general, light scattering measures a collective motion of the particles. However, Weitz and Pine [28] have argued that, for particles larger in diameter than about  $0.4 \mu\text{m}$  (roughly the size of our particles) studied in the DWS limit, the situation simplifies. Then, because of angular averaging over the multiply scattered photon paths, one measures largely the self-motion of the particles, described by their mean square displacements  $\langle \Delta r^2(\tau) \rangle$ . [Of course, the form of  $\langle \Delta r^2(\tau) \rangle$  itself can be strongly affected by interactions in concentrated systems.] Thus we will assume that Eq. (2) applies to our experiments on concentrated systems.

Subjecting a sample to an oscillatory shear strain induces displacements of the particles in addition to those caused by Brownian motion. The echo amplitudes  $g^{(2)}(\tau=mT)-1$ ,

where  $m=1,2,3, \dots$  measure irreversible rearrangements caused by both these influences. Thus we write

$$\sqrt{g^{(2)}(\tau)-1} \approx \exp\left\{-\frac{1}{6}nk^2[\langle \Delta r^2(\tau) \rangle_B + \langle \Delta r^2(\tau) \rangle_S]\right\} \\ \text{with } \tau=mT, \quad (4)$$

where  $\langle \Delta r^2(\tau) \rangle_B$  is the mean square displacement associated with Brownian motion and  $\langle \Delta r^2(\tau) \rangle_S$  is that caused by the shear. The decay of the correlation function  $g^{(2)}(\tau=mT)$ , can therefore be associated with an average shear-induced mean square displacement  $\langle \Delta r^2(\tau) \rangle_S$ . Analysis of the actual shapes of the echoes, described by  $g^{(2)}(\tau)$  at  $\tau \approx mT$ , is a more complicated matter [16]. Here we discuss echo shapes only qualitatively (see Fig. 3 below).

We reiterate the approximate nature of Eq. (4) as applied to our experiments. First, the correlation function measured for dilute systems in transmission DWS [Eq. (2)] is only approximately a single exponential. Second, our experiments are not performed in the strong multiple-scattering limit. Third, under the conditions of our experiments, it may not be possible to neglect collective motions completely.

### III. EXPERIMENTAL SECTION

#### A. Samples

The suspensions consisted of spherical particles of polymethylmethacrylate, sterically stabilized by grafted chains of poly-12-hydroxystearic acid (thickness 10–15 nm), suspended in dodecane. The particles have a radius  $R=183$  nm, and size polydispersity—defined as the standard deviation of the particle size distribution divided by the mean size  $\bar{R}$ ,  $\sigma = \sqrt{\overline{R^2}/\bar{R}^2 - 1}$ —of about 12% as determined by static and dynamic light scattering in dilute suspensions. In agreement with previous experimental and theoretical studies [34,35] such a polydisperse sample does not crystallize at rest. Samples with different particle volume fractions  $\phi$ , ranging from  $\phi=0.58$  to the random close packing (RCP) limit  $\phi=0.67$ , were studied. All samples were prepared by successive dilutions of a RCP sample obtained from centrifugation. Since the suspensions do not crystallize, samples comprising coexisting colloidal fluid and colloidal liquid cannot be used to define the volume fraction. Thus the volume fraction was determined assuming that the sample obtained after centrifugation (at about 1000 g) by removing the supernatant solvent has a volume fraction  $\phi=0.67$ . The latter is an estimate for the volume fraction of randomly close packed polydisperse particles with  $\sigma=0.12$  obtained by computer simulations [36]. The uncertainty of the volume fraction subsequently obtained by dilution is typically  $\pm 0.003$ . The samples were thoroughly mixed and experiments were started immediately after loading the sample.

#### B. Light scattering equipment: Shear cell

A schematic of the shear cell is shown in Fig. 1. It consists of two parallel horizontal glass plates whose separation  $d$  can be adjusted in the range 0.1 to 2 mm. For most experi-

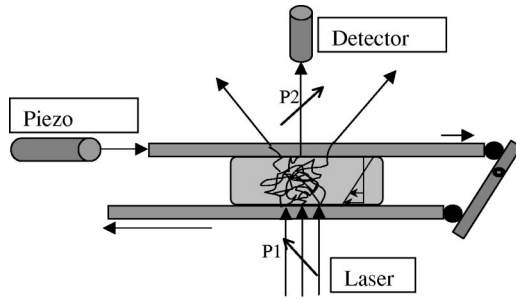


FIG. 1. Schematic of the light scattering echo setup. An air cooled He-Ne laser ( $\lambda = 633$  nm) operating at 25 mW was used to illuminate the sample. The laser beam was unfocused with a diameter of about 2 mm. The scattering is detected in the transmission geometry using a single mode optical fiber and an avalanche photodiode photon counting module. Crossed polarizers (P1 and P2, indicated by two arrows) are used to eliminate single scattering. The shear cell consists of two parallel glass plates with a variable separation. The top plate is directly vibrated by a piezoelectric actuator. The bottom plate is connected to the top one through a lever which amplifies its motion up to about six times. With this arrangement strains of up to 100% can be reached at typical frequency of 70 Hz.

ments presented here the gap was  $d = 0.3$  mm. Both plates are vibrated horizontally using a piezoelectric device at variable frequency  $f (= 1/T)$ , providing a strain  $\gamma = \gamma_0 \sin 2\pi ft$ . In most experiments a frequency of 70 Hz was used. The top plate is driven directly by the piezoelectric actuator with a maximum peak-to-peak amplitude of  $90 \mu\text{m}$ . The other end of the top plate drives a pivoted arm whose bottom end drives the spring-loaded bottom plate in the opposite direction to that of the top plate. The pivoted arm works as a lever enabling the bottom plate to achieve peak-to-peak amplitudes up to about  $600 \mu\text{m}$ . Consequently, the maximum strain amplitude  $\gamma_0 [= 690/(2 \times 300)]$  that could be achieved is about 1.15. Furthermore, in the sheared sample there is a plane, at the level of the pivot, which is stationary in the laboratory frame of reference, a feature that is valuable when studying the samples in a microscope (not reported here). The shear cell is open all the way around and that is why we used a solvent bath to eliminate evaporation by saturating the atmosphere between the parallel plates. The parallelism of the plates was ensured by ball bearings placed between the glass plates. Different sizes of graded ball bearings were used to achieve different separations of the plates. The parallel plates move on precision linear ball bearings to avoid any wobbling during the motion.

The sample is illuminated from below by a helium-neon laser with a wavelength  $\lambda = 633$  nm operating at 25 mW power, while the scattered light is detected above the sample by a single-mode fiber connected to an avalanche photodiode operating in the photon counting mode. A high extinction ratio (better than  $10^{-6}$ ) Glan-Thomson polarizer (from B-Halle) is placed in front of the fiber in the crossed orientation. The polarizer serves two purposes. First, it cuts out any (polarized) single scattering (see below). Second, it ensures that only the depolarized multiple scattering is studied: the polarized and depolarized components of the multiply scattered intensity are uncorrelated and thus, in the absence

of an analyzer in the detection optics, the maximum intercept of the intensity correlation function  $g^{(2)}(0) - 1$  would be decreased by half. Typical measured values of the intensity correlation function (extrapolated to zero delay time)  $g^{(2)}(0) - 1$  were around 0.8, slightly smaller than the ideal value of 1; in the data shown below the correlation functions have been normalized so that  $g^{(2)}(0) - 1 = 1$ . The intensity autocorrelation function was measured using a linear correlator (Flex410R from Correlator.com) which allows an arbitrary distribution of delay channels to be set with great flexibility. The latter is an essential feature in a LS echo experiment where accurate measurement of the echoes requires the clustering of a large number of delay channels around delay times  $\tau = mT$ .

The accuracy and reproducibility of the motion of the parallel plates were tested by measurements in both the strong and weak scattering limits using solid samples including ground glass and white paper. Such samples were attached to the bottom or top plate and oscillated at the typical frequency and amplitude of our experiments. The intensity correlation function measured under such conditions reveals unattenuated echoes of full height up to very high order (echo number of order 100) providing direct evidence for the accuracy and reproducibility of the oscillating motion of the plates.

Concentrated suspensions of PMMA particles in dodecane appear opaque since the difference between the refractive indices of the particles and the solvent is rather high ( $n_D = 1.49$  for PMMA particles and  $n_D = 1.422$  for dodecane). However, for samples with thickness smaller than 2 mm it is found that the condition for DWS approximation does not hold. This is clearly evident since a weak straight-through beam can be seen at such thicknesses. For the sample thickness  $d = 0.3$  mm used in most of our experiments, the straight-through beam typically had an intensity of about 30% of the incident intensity. This implies that the photon mean free path in the sample is roughly equal to the sample thickness itself. Thus, we operate in the regime where the probabilities that a photon is not scattered, is scattered once, or is scattered twice are roughly similar, and there is some probability of higher order scattering. Since the unscattered and single-scattered light is removed by the crossed polarizer (see above) the average number of scatterings  $n$  undergone by the detected photons is a little larger than 2. Other measurements give similar values for  $n$ . For example, for a particular unsheared sample we can estimate  $n$  from Eqs. (1) and (2) when the single scattering is measured by two-color dynamic light scattering, a technique which suppresses multiple scattering [37].

### C. Rheology

A few preliminary rheological measurements were made using two Rheometric Scientific rheometers; a controlled strain ARES-HR with a force balance transducer 100FRTN1 and a controlled stress DSR-200, in a cone-plate geometry (diameter 25 mm and cone angle 0.1 rad). Dynamic strain sweeps were done in the former and step stress (creep) tests in the latter.

#### IV. RESULTS

The particle rearrangements induced by oscillatory shear strain are investigated through measurements in concentrated suspensions of polydisperse hard-sphere particles of different volume fractions in the glass region (volume fraction  $\phi \geq 0.58$ ). The size polydispersity suppresses crystallization of the sample both under quiescent conditions and under shear, enabling the study of shear-induced rearrangements in the absence of ordering transitions. (However, such a shear-induced ordering transition is interesting in itself and will be discussed elsewhere [38].)

Several glassy samples with volume fractions ranging from  $\phi=0.585$  to 0.67 were studied. After loading the sample into the shear cell, a time-averaged intensity correlation function was usually measured for a typical period of half an hour before the commencement of measurements under shear. The intensity correlation function was then measured in the transmission geometry at different strain amplitudes  $\gamma_0$  and at a constant frequency of 70 Hz. The strain was increased progressively with a measurement at each strain lasting about 15 min. Hence, a typical experiment usually lasted not more than 6 h. Since there was concern for effects such as sedimentation or evaporation care was taken to minimize the total time of the experiment. Also, a strain sweep with decreasing strain amplitude was always performed after reaching the maximum strain to ensure the reproducibility of the measurements. At the same time, to avoid evaporation, we used a solvent bath to saturate the atmosphere around the sample.

In general, the response of a glassy system to external forces is expected to depend on the waiting time after the preparation of the sample (aging) [39,40]. In addition, rheological measurements in concentrated suspensions of soft microgel particles [41] have demonstrated mechanical rejuvenation of the system suggesting that aging is interrupted by the application of the appropriate stress as predicted by theory [19]. In our experiments the response of the sample to strain was found to change with time for measurements that lasted more than one day. For example the strain dependence of the echo height was found to be different during the second day after loading the sample. However, since the sample was not density matched we believe that sedimentation played a major role in such a change and thus no genuine aging phenomena could be studied. In the measurements to be described here, all made within a few hours of loading the sample, no time-dependent effects were observed.

##### A. Correlation functions under oscillatory shear

Figure 2 shows the measured intensity correlation function  $g^{(2)}(\tau) - 1$  for two volume fractions under a small strain amplitude. The correlation function initially decays due to the flow-induced motion of the particles and then exhibits narrow peaks (echoes) centered around multiples of the oscillatory shear period  $T$ . The heights of the echoes relate to the amount of reversible motion of particles subjected to oscillatory shear strain. In Fig. 2(a) we show the first ten echoes in the correlation function measured in a random close packed glass under oscillatory shear strain with very

small amplitude ( $\gamma_0=0.008$ ). For such small strains the sample deforms purely reversibly; all particles return to their initial positions after an integral number of oscillations and therefore the heights of all echoes  $g^{(2)}(mT) - 1$  are constant and equal to 1. Figure 2(b) displays the intensity correlation function from a less concentrated sample ( $\phi=0.587$ ) under periodic strain with amplitude  $\gamma_0=0.019$  where echoes 1–4, 21, and 22 are shown. Here the restricted Brownian motion of the particles inside the cage ( $\beta$  relaxation) is revealed in the decay of  $g^{(2)}(\tau)$  in the absence of shear. For such low strain amplitude the peaks of the echoes exhibit the same decay as in the absence of shear, verifying that there are no irreversible rearrangements additional to those caused by Brownian motion.

Under multiple scattering conditions, the initial decay of  $g^{(2)}(\tau)$ , related to the Brownian motion of particles inside their cage, is speeded up relative to that measured by single scattering by a factor  $n$  [compare Eqs. (1) and (2)]. Indeed, at the limit of very large  $n$  (thick samples)  $g^{(2)}(\tau)$  appears ergodic [ $g^{(2)}(\tau) - 1$  tends to zero at large  $\tau$ ] since the characteristic length scale probed,  $l_{DWS}$ , is smaller than the maximum excursion of the particle in a cage and hence local in-cage motions lead to a complete decay of the correlation function. Thus, in order to be able to detect at least one echo in the correlation function, the apparent long relaxation time  $\tau_l^m$  under multiple scattering conditions must be larger than the period  $T$  ( $=1/f=0.0143$  s for  $f=70$  Hz) of the shear ( $\tau_l^m > T$ ). For all volume fractions of the colloidal glasses studied here (e.g., Fig. 2) we have  $\tau_l^m > T$  but  $\tau_s^m \leq T$ , where  $\tau_s^m$  is the apparent short relaxation time.

When assessing the relative importance of Brownian motion and shear, as described by the Péclet number (see Sec. I), we must use the intrinsic relaxation times of the system rather than those measured in (multiple) light scattering. Here we can refer to the measurements by van Meegen *et al.* [39] of mean square displacements in concentrated suspensions of PMMA particles. They find that at  $\phi=0.583$  particles start to be affected by the surrounding cage at about  $1.6\tau_{B,0}$  (see Fig. 7 of Ref. [39]) with  $\tau_{B,0}=R^2/2D_0$  being the Brownian time of a dilute suspension. If we use this value in the calculation of the Péclet number for our system, we find that for strain amplitudes  $\gamma_0$  0.1 to 1 we get  $Pe=0.1-1$  (taking the maximum strain rate to be  $f\gamma_0$ ). However, employing the time at which the mean square displacement reaches the intermediate plateau between the short-time diffusion (in-cage motion) and the long-time diffusion (motion between cages) [39],  $\tau_B \approx 400\tau_{B,0}$ , the resulting Péclet number is  $Pe=25-250$ . These estimates suggest that the shear strain imposed in our experiments distorts significantly the metastable equilibrium structure of the glass related to long range frozen density fluctuations, while the local, in-cage particle distribution function remains relatively unaffected.

The correlation function for the lower volume fraction ( $\phi=0.587$ ) is plotted in Fig. 3 for different shear strains. The initial decay and the first echo are shown. In contrast to higher volume fractions, here the decay of the echoes is affected by the Brownian motion of the particles since the short relaxation time  $\tau_s^m$  measured under multiple scattering

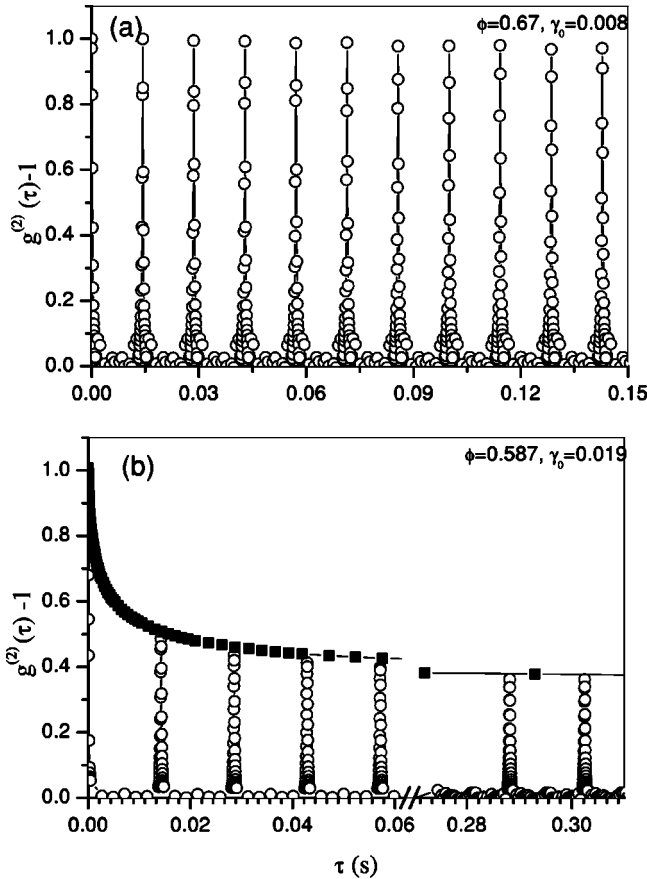


FIG. 2. Correlation functions under oscillatory shear ( $f = 70$  Hz) at low strain amplitudes (a) for the random closed packed ( $\phi = 0.67$ ) sample (no Brownian motion) under oscillatory shear; echoes 1–10 are shown (○) for a strain amplitude  $\gamma_0 = 0.008$ . (b) Echoes 1–4 and 20, 21 are shown for a low volume fraction glass ( $\phi = 0.587$ ) sample at a low strain  $\gamma_0 = 0.003$ , (○). The sample strains elastically as indicated by the unattenuated echo heights which follow the correlation function measured in quiescent conditions (■).

conditions is similar to the period of the oscillatory shear. With increasing strain  $\gamma_0$ , the initial decay of the correlation function, arising from the deterministic motion due to the shear flow, speeds up while the echo becomes narrower. The width of the echo (at half height) is twice the initial decay time  $\tau_{ini}$ , and directly proportional to the inverse strain rate ( $1/\dot{\gamma}$ ) [16]. The linear dependence of the initial decay rate  $\Gamma (= 1/\tau_{ini})$  on strain amplitude shown in the inset of Fig. 3 verifies the absence of wall slip in our measurements. Such linear dependence of  $\Gamma$  on  $\gamma_0$  is observed in all volume fractions, similar to the case of concentrated emulsions [16] but contrary to the case of sheared foam [17] where a crossover from linear to nonlinear periodic displacements was observed.

In Fig. 4 the envelope formed by the echo peaks at different strain amplitudes is shown for a high ( $\phi = 0.626$ ) and a low ( $\phi = 0.587$ ) volume fraction sample. For low strains,  $g^{(2)}(mT)$  reflects the dynamics of the unsheared sample [as in Fig. 2(b)]. As strain is increased, shear-induced irrevers-

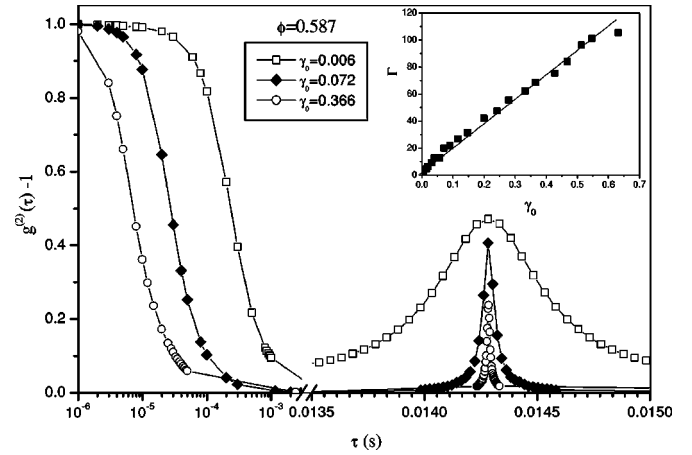


FIG. 3. Correlation functions for the lower volume fraction glass sample ( $\phi = 0.587$ ) (which shows Brownian motion) under oscillatory shear ( $f = 70$  Hz). The initial decay and the first echo are shown for three different strain amplitudes:  $\gamma_0 = 0.006$  (□),  $\gamma_0 = 0.072$  (◆), and  $\gamma_0 = 0.366$  (○). Inset: Strain dependence of the initial decay rate; the solid line indicates the linear increase of  $\Gamma$  with  $\gamma_0$ .

ible rearrangements (yield) cause a drop of the echoes. Furthermore, above the onset of yield a further decay of the higher order echoes is observed. To illustrate this behavior better we plot in Fig. 5 the ratio of the field correlation function  $g^{(1)}(mT) = \sqrt{g^{(2)}(mT) - 1}$  to that at the lowest measured strain, for the two volume fractions shown in Fig. 4. It is now clear that, both at high and low volume fractions, oscillatory shear at a strain above the onset of yield induces a decay of high order echoes. This behavior is in contrast with the observations of Hébraud *et al.* [16] in highly concentrated emulsion glasses where high order echoes were found to retain the same amplitude as the first one at all strains. Here we find that hard-sphere colloidal glasses exhibit a different response to shear. We may relate the temporal decay of the echoes in  $g^{(1)}(mT)$  to an average shear-induced diffusion rather than to a ratio of particles that return to their initial position. Moreover, for times between 0.05 and 0.4 s the echo peaks seem to level to a plateau that decreases with increasing shear strain (Fig. 5). This plateau can be interpreted as the shear-induced value of the nonergodicity parameter,  $f^{(\infty)} [= g^{(1)}(\infty)]$ .

Figure 6 shows the decay of the first and 21st echoes with increasing and decreasing strain amplitude for the lowest volume fraction  $\phi = 0.587$ , which is still a glass. The echo amplitude is represented by the ratio of the intensity correlation function  $g^{(2)}(mT) - 1$  at a multiple of the oscillation period (here  $m = 1$  and 21) to  $g^{(2)}(0) - 1$ . Upon increasing or decreasing the strain the sample responds in exactly the same way, as suggested by the essentially identical echo amplitudes. Such reproducibility of the data is observed in all measurements at different volume fractions, verifying that the samples are not aging significantly nor crystallizing. Note that similar experiments in significantly less polydisperse samples ( $\sigma = 0.06$ ) reveal shear-induced ordering causing hysteresis effects in the measured echo heights [38].

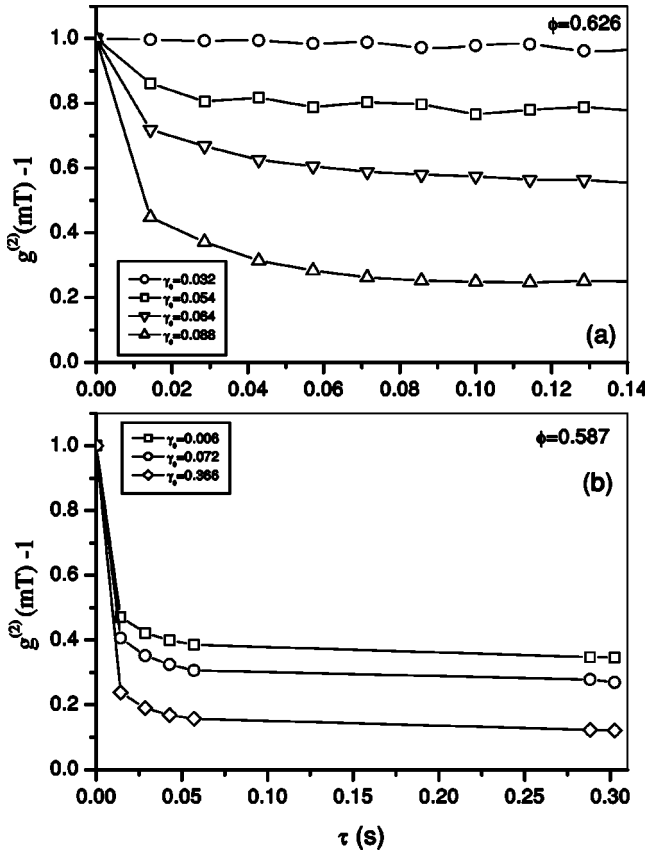


FIG. 4. The envelope of the correlation function formed by the peaks of the echoes is shown for various strain amplitudes. (a) For a  $\phi=0.626$  glass, at  $\gamma_0=0.032$  ( $\circ$ ),  $\gamma_0=0.054$  ( $\square$ ),  $\gamma_0=0.064$  ( $\nabla$ ), and  $\gamma_0=0.088$  ( $\triangle$ ). (b) For the less concentrated glass with  $\phi=0.587$ , at  $\gamma_0=0.006$  ( $\square$ ),  $\gamma_0=0.072$  ( $\circ$ ), and  $\gamma_0=0.366$  ( $\diamond$ ).

### B. Volume fraction dependence

The strain amplitude dependence of the first echo, represented by  $[g^{(2)}(T) - 1]/[g^{(2)}(0) - 1]$ , is shown in Fig. 7 for several volume fractions. In the RCP sample ( $\phi=0.67$ ) particle dynamics are completely frozen and the correlation function of the quiescent sample does not show evidence of any in-cage short time dynamics. Under shear the sample starts to yield at very low strains ( $\gamma_0 \approx 0.01$ ), and shear-induced irreversible rearrangements increase strongly with strain resulting in a sharp drop of the echo amplitude. Glasses at lower volume fractions respond almost reversibly up to a characteristic strain  $\gamma_0 = \gamma_{c1}$ , as indicated by the initial plateau of  $[g^{(2)}(T) - 1]/[g^{(2)}(0) - 1]$ . Above  $\gamma_{c1}$  shear induces irreversible rearrangements and the sample starts to yield. The effect of the Brownian motion on the amplitude of the first echo is seen in the drop of the values of  $[g^{(2)}(T) - 1]/[g^{(2)}(0) - 1]$  at  $\gamma_0 \rightarrow 0$ . In contrast to the RCP solid sample, at lower  $\phi$  the fast particle diffusion in the cage is clearly detectable [Figs. 2(b) and 3] and is responsible for the drop of the intercept indicated by the arrows in Fig. 7. The values of  $[g^{(2)}(T) - 1]/[g^{(2)}(0) - 1]$  at  $\gamma_0 \rightarrow 0$  for all volume fractions are plotted in the inset of Fig. 7. Increasing the volume fraction, the  $\beta$  relaxation becomes weaker as the particles are increasingly restricted in tighter cages.

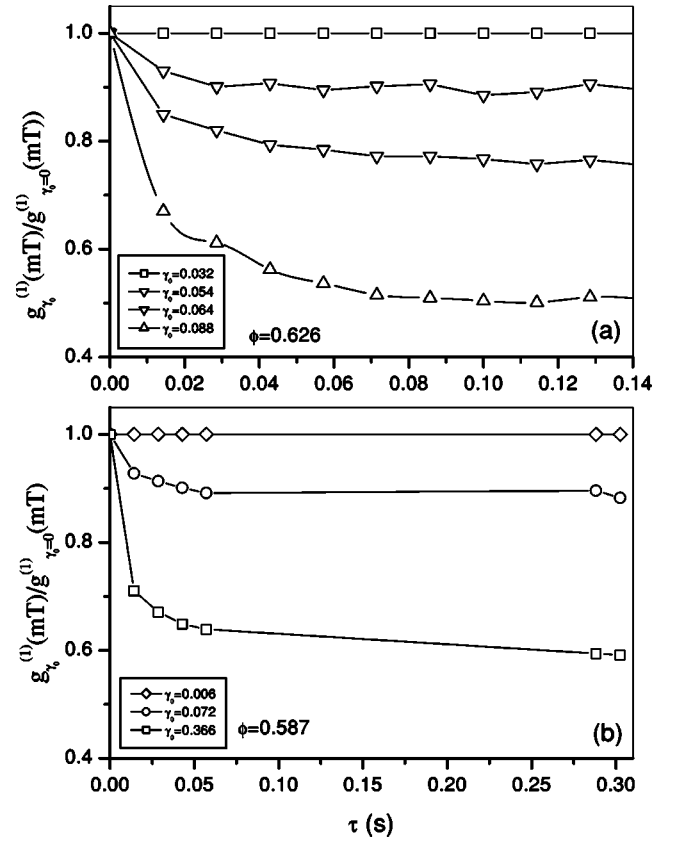


FIG. 5. The decay of high order echoes at various strain amplitudes is represented by the ratio of the amplitude of the  $m$ th echo to a strain  $\gamma_0$  to the corresponding amplitude at the lowest strain,  $g_{\gamma_0}^{(1)}(mT)/g_{\gamma_0=0}^{(1)}(mT)$ . This ratio takes into account the decay of the high order echoes due to Brownian motion, which is increasingly important upon lowering the volume fraction. (a) A high (0.626) and (b) a low (0.587) volume fraction are shown.

In order to concentrate just on shear-induced rearrangements, we define

$$P \equiv \sqrt{g^{(2)}(\tau) - 1} \quad \text{for } \tau = mT \quad (5)$$

and consider the quantity  $P/\lim_{\gamma_0 \rightarrow 0} P$ , which measures the amplitude of the echo at a certain strain relative to its amplitude at low strain. At low strain amplitudes this quantity has a value 1, and any reduction from 1 reflects only irreversible shear-induced rearrangements. From Eqs. (4) and (5) we get

$$P/\lim_{\gamma_0 \rightarrow 0} P \approx \exp\left\{-\frac{1}{6}nk^2\langle\Delta r^2(mT)\rangle_S\right\}. \quad (6)$$

The effect of oscillatory shear, measured by the quantity  $P/\lim_{\gamma_0 \rightarrow 0} P$  for the first echo ( $\tau = T$ ), is shown in Fig. 8 as a function of  $\gamma_0$  for glasses at volume fractions ranging from  $\phi=0.67$  (RCP) to  $\phi=0.587$ . The onset of irreversible rearrangements,  $\gamma_{c1}$ , and the characteristic strain at which the echo has disappeared,  $\gamma_{c2}$ , are indicated by vertical arrows. Figure 8 reveals a qualitatively different response of the glass as volume fraction increases. As discussed further below, two regimes of behavior, with different dependences on

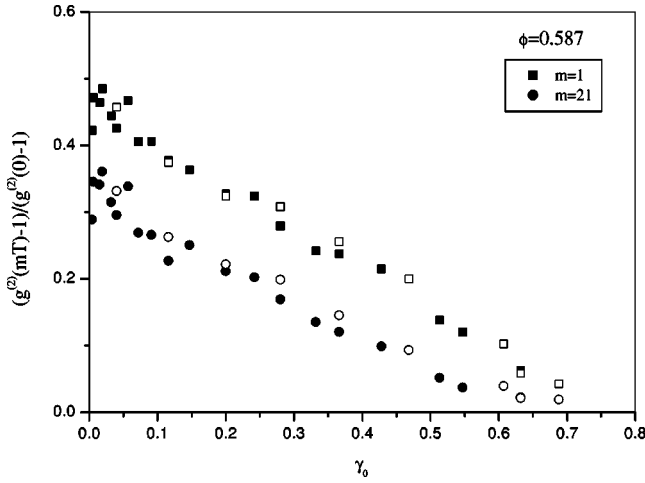


FIG. 6. Strain amplitude dependence of the echo amplitude  $g^{(2)}(mT) - 1$  normalized only to the intercept of the correlation function,  $g^{(2)}(0) - 1$ . The amplitudes of the first (squares) and 21st (circles) echoes are shown for an increasing (solid symbols) and decreasing (open symbols) strain sweep at a volume fraction of 0.587. The reproducibility of the results suggests that there are no structural changes in the sample during this cycle.

strain, can be identified. (i) At relatively high volume fractions the glass behaves reversibly under small oscillatory shear strains, as indicated by the plateau at  $P/\lim_{\gamma_0 \rightarrow 0} P \approx 1$ . Above  $\gamma_{c1}$  the echo amplitudes drop quite rapidly, signaling the onset of irreversible rearrangements (yield). The characteristic strain  $\gamma_{c1}$  increases with decreasing volume fraction from 0.01 at RCP to about 0.15 at  $\phi = 0.623$ . (ii) At somewhat lower concentrations, yielding starts at lower strains, but the echo amplitudes decrease comparatively more slowly with increasing strain (e.g., Figs. 7 and 8 for  $\phi = 0.587$ ). Consequently, at large strain amplitudes, low  $\phi$

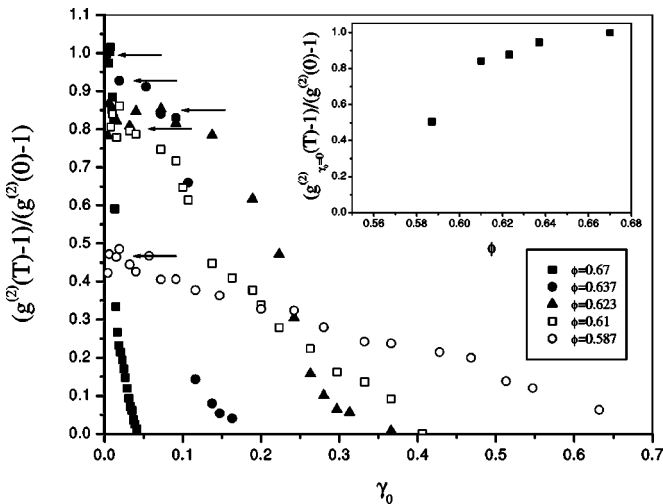


FIG. 7. Strain amplitude dependence of the amplitude of the first echo,  $g^{(2)}(T) - 1/g^{(2)}(0) - 1$ , for all volume fractions as indicated. The arrows point at limiting values at zero strain,  $[g^{(2)}(T) - 1/g^{(2)}(0) - 1]_{\gamma_0=0}$ , which relates with the contribution of the Brownian motion in the decay of  $g^{(2)}(T)$ . Inset: Volume fraction dependence of  $[g^{(2)}(T) - 1/g^{(2)}(0) - 1]_{\gamma_0=0}$ .

glasses respond more reversibly than those at high  $\phi$ . We return to discuss these observations further in the next section.

Figure 9 shows the volume fraction dependence of the two characteristic strains  $\gamma_{c1}$  and  $\gamma_{c2}$ . Their  $\phi$  dependence reflects the qualitatively different yielding behavior of low and high volume fraction glasses (Fig. 8). Whereas the onset of yield  $\gamma_{c1}$  follows a nonmonotonic dependence on  $\phi$ , the characteristic strain  $\gamma_{c2}$  at which the sample does not exhibit any reversible response (so that the sample may be considered totally fluidized) decreases continuously with increasing  $\phi$  toward RCP.

Since the echo drop originates from shear-induced irreversible rearrangements measured over a length scale determined by the scattering conditions it might exhibit different strain dependence if the number of scattering events is altered. If we probe large length scales ( $\geq 10R$ ) by small-angle single scattering we would not be able to detect irreversible rearrangements at a subparticle level and thus the echo would decay at higher strains. However, for an ideal elastic solid it should be expected that the critical strain  $\gamma_{c1}$  would not depend on the probing length scale provided that the latter is smaller than the former.

The ratio of the shear-induced root mean square displacement to the particle diameter,  $\langle \Delta r^2(T) \rangle_S^{1/2}/2R$ , determined according to Eq. (6) at  $\tau = T$  is shown in Fig. 10 for all volume fractions as a function of strain amplitude. In the calculation of  $\langle \Delta r^2(T) \rangle_S$  we assumed the number of scatterings  $n$  to be 2 (see Sec. III B). Under these effectively double-scattering conditions, particle rearrangements on the length scale of a particle radius or smaller can be followed.  $\langle \Delta r^2(T) \rangle_S^{1/2}/2R$  is the shear-induced enhancement of particle displacement after one period of oscillation. At high volume fractions, after the initial region of almost reversible motion,  $\langle \Delta r^2(T) \rangle_S^{1/2}/2R$  increases rapidly with  $\gamma_0$ , implying abrupt shear-induced rearrangement. At  $\phi = 0.61$  the dimensionless shear-induced displacement is (probably coincidentally) almost exactly the same as the imposed strain. That is to say, the irreversible displacement of a particle over one cycle is more or less equal to the distance that it moves relative to its nearest neighbors in one cycle of imposed strain. [However, for the reasons discussed at the end of Sec. II, one should not place too much reliance on the exact numerical values of  $\langle \Delta r^2(T) \rangle_S^{1/2}/2R$  in Fig. 10.]

## V. DISCUSSION

We start the discussion with some general observations about flow in concentrated suspensions of hard-sphere particles which, at first sight, might seem counterintuitive—or, at least, surprising. For simplicity we assume that sedimentation can be neglected.

Consider first a suspension of hard spheres in which Brownian motion is hypothetically absent (approximated by a suspension of large enough neutrally buoyant particles). Without applied stress, the particles do not move. If a steady shear stress is applied, the suspension flows. For hard spheres, the only interactions (apart from volume exclusion) between the particles are hydrodynamic interactions trans-

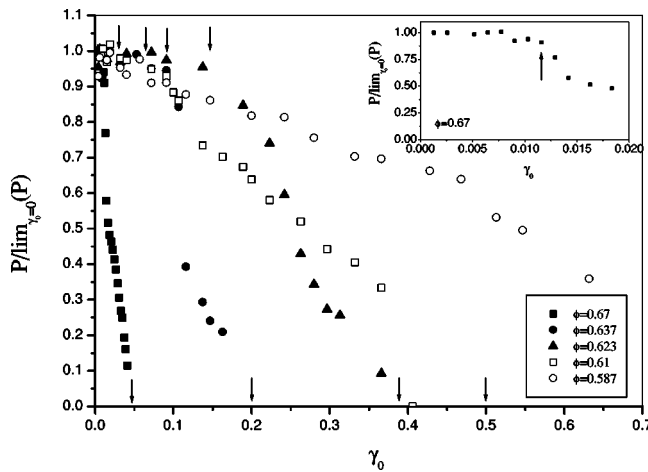


FIG. 8. Strain dependence of the relative first echo height ( $P/\text{lim}_{\gamma_0 \rightarrow 0} P$ ) at several volume fractions as indicated. As described in the text, presenting the data in this form removes the effect of Brownian motion. Thus, when  $P/\text{lim}_{\gamma_0 \rightarrow 0} P = 1$  the sample strains elastically, and any reduction below 1 implies irreversible shear-induced rearrangements. The inset shows the data for the random close-packed sample with an expanded  $x$  axis.

mitted through the liquid. As shown, for example, by the simulations of Brady and Morris [22] and Melrose *et al.* [13], such a suspension will, at any concentration, eventually jam when clusters of particles, brought together by the flow and then bound by the strong hydrodynamic lubrication forces, span the sample container. At high particle concentrations, jamming occurs “quickly,” i.e., after the sample has undergone a small strain; at lower concentrations, larger strains can be tolerated before jamming. Now consider reversing the direction of the shear stress before jamming occurs. An important property of hydrodynamics at low Reynolds number (“Stokes flow”) is that the equations of motion are reversible. Thus, on reversing the shear stress, the particles will exactly retrace their earlier trajectories, and will eventually return to their original positions [42]. Therefore, in the absence of Brownian motion and provided that jamming is avoided, the motions of suspended particles are completely reversible even though the sample may undergo large strains, i.e., initially neighboring particles may become widely separated before the stress is reversed.

Now consider a suspension in which Brownian motion of the particles is significant, e.g., small particles. Even without stress applied, the particles will, of course, move. At low to moderate concentrations, in the fluid state of the sample, any particle can, given enough time, diffuse throughout the sample container. However, above the concentration of the glass transition, volume fraction  $\phi \approx 0.58$ , the particles are more or less permanently caged by their neighbors, able only to execute small Brownian excursions in the free volumes within their cages. On further increase of the concentration to random close packing,  $\phi \approx 0.67$ , each particle is in permanent contact with several others and there is no free volume for local motions: the particles do not move and the sample is clearly a solid. Under an applied stress, this sample can only yield by dilating, increasing its volume (and drawing in

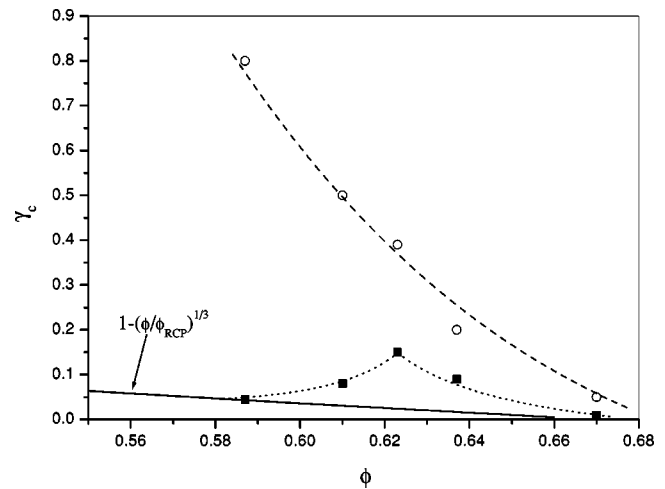


FIG. 9. The volume fraction dependence of the critical strains  $\gamma_{c1}$  (■) and  $\gamma_{c2}$  (○), determined from the curves in Fig. 8 as the strain values, where irreversible rearrangements first appear and result in complete decay of the first echo, respectively. The dashed and dotted lines are to guide the eye. The solid line represents the critical strain  $1 - (\phi/\phi_{RCP})^{1/3}$ , related to the surface-surface interparticle distance.

air), to give the particles space to move. At a slightly lower concentration the particles have small free volumes within which their centers can move. Yet it is a fact of experience, surprising considering that the free volumes may be only 1% or 2% of the particles’ actual volume, that if such a sample is subjected to a small stress, for example, the gravitational stress induced by tipping its container, it will flow without visible dilation, albeit very slowly. Apparently, although in the absence of stress the particles are permanently caged by their neighbors (the sample is solid), it requires only a small stress to break the cages and allow flow. Given the very small free volumes available to them, the particles must follow tortuous, highly correlated, trajectories to get past each other.

Note, also, that the observation of flow in concentrated samples at low stress implies that jamming does not occur, as it would in the absence of Brownian motion (see above). In fact, it is known that at larger stresses the sample does jam. This is illustrated directly by the “cornstarch experiment.” A concentrated suspension of cornstarch in water can be gently stirred by a spoon, and flows smoothly; but, if vigorous stirring is attempted, the suspension jams and solidifies. This behavior is understood in terms of competition, quantified by a Péclet number, between stress-induced flow and Brownian motion (discussed in Sec. I). At a large enough Péclet number, stress-induced motion dominates and the suspension jams as it would in the complete absence of Brownian motion. However, at small Péclet numbers random Brownian displacements apparently prevent jamming and allow the suspension to flow.

From these observations we reiterate three important points. (1) In the absence of Brownian motion, the motions of particles in a sheared suspension are completely reversible. (2) In the absence of Brownian motion, a sheared suspension will jam. (3) At low Péclet numbers, Brownian mo-

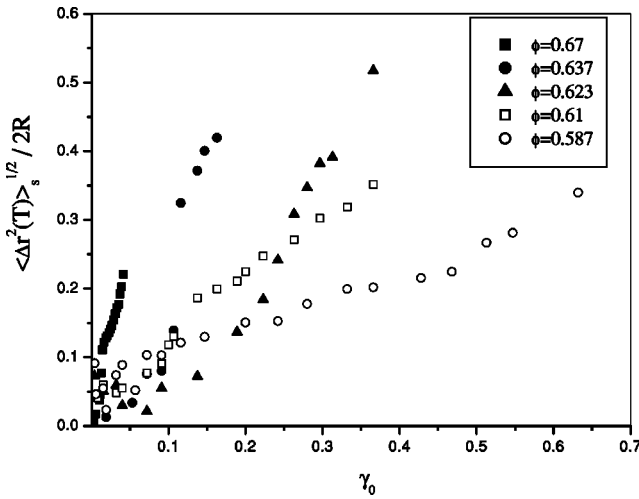


FIG. 10. Square root of the shear-induced mean square displacements normalized to the particle diameter,  $\sqrt{\langle \Delta r^2(\tau) \rangle_s} / 2R$ , as a function of strain amplitude for various volume fractions as indicated.

tion prevents jamming, and allows flow even at very high suspension concentrations. We now consider the implications of these points for the interpretation of our experiments. First it is clear that there are different kinds of distortion of a sample which can lead to the observation of light scattering echoes under oscillatory shear. One is an elastic distortion, where the strain of the sample would spontaneously return to zero if the stress were removed. Another is what might be called a reversible viscous distortion, of the kind discussed above, which results from the reversibility of the hydrodynamic equations. Here, if the stress is removed at some time, the sample will retain the distortion that it has accumulated up to that time; only if the stress history is reversed will the particles in the sample regain their original positions. Second, it is also clear that, although detailed analysis may be difficult, light scattering echo experiments should provide information on the complicated way in which stress-induced and Brownian motions interact in the flow of concentrated suspensions. The experimental behavior can, in fact, be viewed as a high concentration analog of Taylor dispersion in dilute suspensions, where diffusional spread of particles in the direction of a steady shear flow is enhanced by their transverse diffusion into different streamlines. Furthermore, combining LS echo and rheology should help to distinguish between elastic and reversible viscous responses. Below we attempt to rationalize the experimental findings presented in Sec. IV in the light of these remarks.

Interpretation of the results (Fig. 8) for the random close-packed  $\phi=0.67$  sample seems straightforward. This sample is a quite stiff paste, formed in a centrifuge tube at an acceleration of  $\sim 1000g$  and then carefully transferred to the shear cell. The PMMA particles (radius 183 nm) are sterically stabilized by coatings (thickness 10–15 nm) of a polymer brush of poly-12-hydroxystearic acid. In the RCP sample any one particle is touching several others, randomly arranged around it, so that their coatings overlap. The coatings are somewhat elastic, so that this amorphous solid can tolerate some elastic

strain. The results of Fig. 8 (inset), where the plateau at  $P/\lim_{\gamma_0 \rightarrow 0} P \approx 1$  extends to a strain of about 0.01, imply an elastic response corresponding to a compression of the particles' coatings by about 3 nm. For  $\gamma_0 \geq 0.01$ , the amorphous solid dilates and visible cracks appear: the rapid drop of the echo amplitudes toward zero with increasing  $\gamma_0$  implies significant irreversible rearrangements within the sample.

Consider now the samples at slightly lower concentrations  $\phi=0.637$  and 0.623. In these samples, the particles are not touching on average, and undergo restricted Brownian motion inside the cages formed by their neighbors. An estimate of the average separation of the surfaces of two neighboring particles is  $2R[(\phi_{RCP}/\phi)^{1/3}-1]$  (where  $2R$  is the average diameter of the particles), or  $\sim 0.025 \times 2R$  for  $\phi=0.623$ . Naively, therefore, one might expect that this sample could tolerate an elastic strain of  $\gamma_0=0.025$ , and that for strains larger than this the particles would bump into each other, inducing irreversible rearrangements. In fact the data of Figs. 8 and 10 suggest much larger characteristic strains than this: the plateau where  $P/\lim_{\gamma_0 \rightarrow 0} P \approx 1$  extends to  $\gamma_{c1} \approx 0.1$  for  $\phi=0.637$  and to  $\gamma_{c1} \approx 0.15$  for  $\phi=0.623$ . Thus the introduction, by dilution from RCP, of a small amount of free volume into the sample allows a much larger reversible distortion than the naive estimate suggests. The detailed mechanism by which this occurs is uncertain but, in view of the discussion above, both elastic and reversible viscous effects are likely to contribute. To picture the elastic component, one could imagine that the cluster of 10 or 12 particles, which make up a particle and its cage, could be distorted considerably under oscillatory shear without the particles significantly changing their relative positions. By contrast with the “particle elasticity” exhibited by the RCP sample, one might call this behavior “cage elasticity.”

The behavior exhibited by the samples at  $\phi=0.61$  and 0.587 [type (ii) behavior, Sec. IV] implies more gradual shear-induced structural change: irreversible rearrangement starts at lower strain amplitudes but memory of the initial structure persists to higher amplitudes. Again a main issue is to separate elastic and viscous effects. One might speculate that the high strain reversibility is largely viscous in nature, since it is difficult to believe that a particle cage would retain its integrity under strains as large as  $\gamma_0=0.5$ . Here, preliminary rheological measurements can shed some light—so far we only have data on a low concentration glass  $\phi=0.584$ . Figure 11(b) shows a step stress (creep) experiment. A small constant stress ( $5 \text{ dyn/cm}^2$ ) is applied for 60 s and the resulting strain is monitored for 250 s. As can be seen in the figure, the maximum strain achieved is about 0.08. When the stress is removed, the sample recovers elastically a strain of about 0.03, leaving an unrecovered strain of about 0.05. Yet Fig. 8, for  $\phi=0.587$ , shows that, for a strain amplitude  $\gamma_0=0.08$ , the particle motions under oscillatory shear are almost completely reversible ( $P/\lim_{\gamma_0 \rightarrow 0} P \approx 0.9$ ). We can conclude, therefore, that a large part of the strain which is not recovered in the rheological measurement is associated with a reversible viscous distortion on the time scale of the light scattering echo measurements.

Figure 11(a) shows, for the same sample at  $\phi=0.584$ , a

dynamic strain sweep which resembles the rheological conditions under which the LS echo experiments were performed. The storage  $G'$  and loss  $G''$ , moduli were measured along with the complex viscosity  $\eta^*$ , as function of strain amplitude at a frequency of 10 Hz. At low strains  $G'$  is greater than  $G''$ , consistent with the sample showing some true elasticity. For strains  $\gamma_0 > 0.20$ ,  $G'$  and  $G''$  are similar, indicating that the sample is viscoelastic. (A more complete study of the macroscopic rheological properties of polydisperse hard-sphere glasses will be presented elsewhere [43].)

Returning to the nature of cage elasticity, we look again at measurements by van Meegen *et al.* [39] of the Brownian mean square displacements of particles measured in similar PMMA colloidal glasses under quiescent conditions. These authors found that, in a low volume fraction colloidal glass ( $\phi = 0.58$ ), the mean square displacement  $\langle \Delta r^2(\tau) \rangle_B / R^2$  saturates at about 0.08 so that  $\sqrt{\langle \Delta r^2(\infty) \rangle_B} = 0.28R$ . In other words, although the distance between neighboring particle surfaces is small (about  $0.067R$ ), a particle can move over distances of  $0.28R$  while still in its cage. Such a large range of motion of a single particle implies quite loose cages and strongly collective motions of groups of particles. This observation is consistent with the surprisingly large reversible cage distortions discussed above.

The discussion so far has concentrated on the behavior of the first echo as a function of strain amplitude at several volume fractions. In addition, the higher order echoes monitor the dependence of the slow dynamics on shear strain. Thus the temporal decay of the echo peaks describes the effect of oscillatory shear strain on the slow  $\alpha$  relaxation, associated with the restructuring of the cage. The fact that there is a temporal decay of the high order echo (see Fig. 5) supports the notion of a speedup of the slow dynamics due to shear. Such dependence on shear strain is reminiscent of the behavior of the correlation function in glassy systems driven by an external force suggested by theory and simulations by Berthier *et al.* [19]. The correlation functions of high volume fraction samples at very low strains exhibit a plateau at times up to 0.1–1 s corresponding to the frozen fluctuation of the glass [Fig. 4(a)] with a nonergodicity parameter of almost 1. At higher strains, the echoes reveal a temporal relaxation toward a plateau which decreases with increasing strain; finally, above the characteristic strain  $\gamma_{c2}$  the sample flows and the correlation function completely decays to zero at 0.1–1 s. At lower volume fractions the observed decay of the echoes at low strains [Fig. 4(b)] results from the Brownian motion of the particles in their cages. On increasing the strain, however, the observed dynamics again speed up further [Fig. 4(b)]. If the contribution of the Brownian motion is divided out (Fig. 5), a qualitatively similar behavior is revealed for all volume fractions. Furthermore, as is the case for the first echo (above), higher order echoes do exhibit a more gradual decay with strain at lower volume fractions.

Thus, hard-sphere colloidal glasses do not exhibit the “localized yielding” effect found in concentrated emulsions under shear [16], where two independent sets of particles undergo either reversible or chaotic motion and the high order echoes all retain the same amplitude as the first. In our case it seems more appropriate to discuss the decay of high order

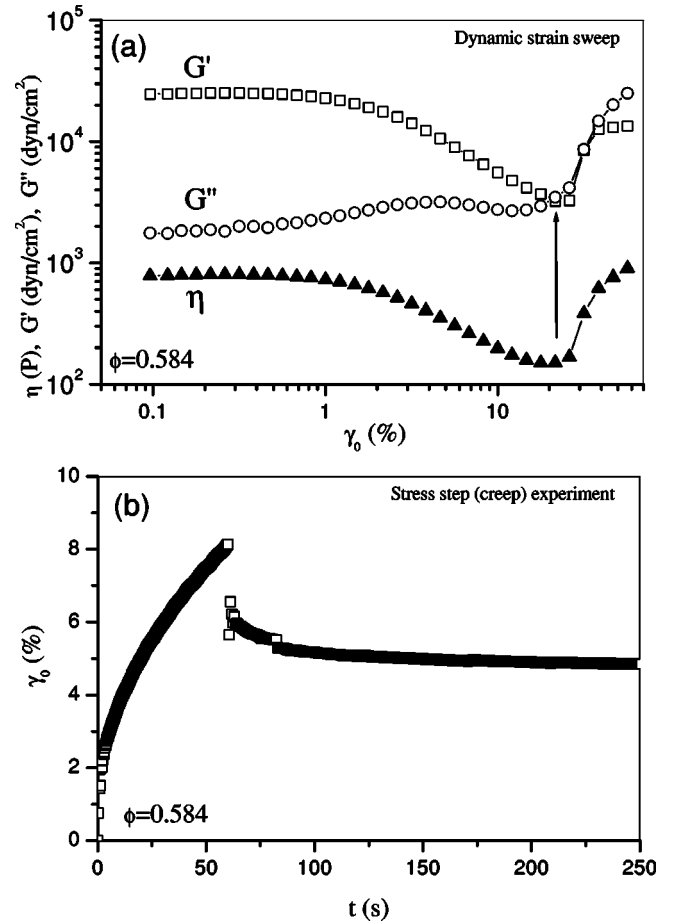


FIG. 11. (a) Strain dependence of the dynamic shear moduli (storage  $G'$ ,  $\square$ ; loss  $G''$ ,  $\circ$ ) for a low volume fraction glass at a frequency of 10 Hz. The  $G'$ - $G''$  crossover, shown by the arrow, identifies the yield strain. The complex dynamic shear viscosity  $\eta^*$  is also shown in the plot ( $\blacktriangle$ ). (b) Stress step (creep) experiment at a stress  $\sigma = 5$  dyn/cm<sup>2</sup>.

echoes in terms of a shear-induced diffusion, analogous to a high volume fraction Taylor dispersion.

Finally, we mention that LS echo measurements performed as a function of frequency should provide valuable information about the interaction between Brownian motion and shear flow. As discussed at the beginning of this section, in the absence of Brownian motion, particle trajectories should be completely reversible. With Brownian motion, however, any particle will generally end up after half a cycle of shear in a different position than would have been the case without Brownian motion. Thus in the next half cycle it will not follow in reverse exactly its initial trajectory. The greater the Brownian displacement, the more different will be the initial and reverse trajectories. At higher oscillation frequencies, the particles have less time to move in Brownian motion during one cycle; therefore the induced flow in the sample should be more reversible and the measured light scattering echoes should be larger. Preliminary measurements show this to be the case. Figure 12 shows the strain amplitude dependence of the first echo, represented by  $[g^{(2)}(T) - 1] / [g^{(2)}(0) - 1]$ , for two different frequencies ( $f = 10$  Hz and  $f = 70$  Hz) at a volume fraction  $\phi \approx 0.625$ . In

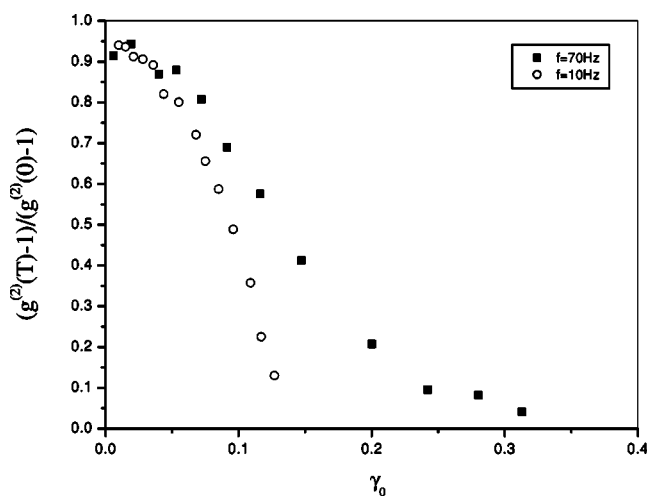


FIG. 12. Strain amplitude dependence of the first echo amplitude at two different frequencies at  $f=70$  Hz (■) and  $f=10$  Hz (○). The volume fraction of the sample is  $\phi \approx 0.625 \pm 0.005$ .

these measurements it is clear that the echo amplitudes are smaller at the lower frequency ( $f=10$  Hz). Thus, the irreversible rearrangements in the sample are, because of Brownian motion, greater as the frequency of oscillatory shear is decreased.

## VI. CONCLUSIONS

The qualitative features of shear-induced rearrangements and ordering can be studied by the light scattering echo technique, providing quantitative microdynamic information on the yielding process. Under oscillatory shear colloidal glasses can sustain surprisingly large strains, up to about 15%, before they start yielding irreversibly. The results presented here suggest that concentrated particle suspensions yield in a quite complicated manner under the application of shear.

The nature of the yielding process depends strongly on concentration. At high volume fractions ( $\phi \gtrsim 0.62$ ), irreversible rearrangements increase rapidly as strain amplitude is increased while at lower volume fractions a more gradual yielding is observed. Such complicated behavior results from a combination of three effects: an elastic distortion, as measured in rheological experiments; a reversible viscous distortion; and a high concentration analog of Taylor dispersion arising from the interplay of Brownian motion and Stokes flow.

Following the high order echoes with increasing strain we are able to monitor the strain dependence of the frozen-in fluctuations in the glass. Their decay with increasing echo number represents the speeding up of the long time relaxation ( $\alpha$  relaxation) as the external drive is increased, eventually leading to a shear-induced fluidization of the glass at high strain amplitudes.

There are several clear directions in which this research can be developed. Further comparison between rheological and light scattering echo measurements should allow a more complete separation of elastic and reversible viscous distortions. More extensive LS echo measurements as a function of frequency should elucidate the interplay of Brownian motion and Stokes flow. Finally, it might be possible to follow directly in a microscope the tortuous trajectories followed by particles in sheared concentrated suspensions.

## ACKNOWLEDGMENTS

We thank Mike Cates, Matthias Fuchs, Stefan Egelhaaf, Wilson Poon, and Daan Frenkel [43] for useful discussions. We also thank Dimitris Vlassopoulos and the Institute of Electronic Structure and Lasers—FORTH (Crete) for the rheological measurements, and Andrew Schofield for the synthesis of the PMMA particles. G.P. acknowledges funding by the European Community program under Contract No. ERBFMBICT983380. The work was also funded by Grant No. GR/M06239 of the U.K. Engineering and Physical Sciences Research Council and by Unilever Research.

- 
- [1] B. J. Ackerson and P. N. Pusey, *Phys. Rev. Lett.* **61**, 1033 (1988).
  - [2] B. J. Ackerson, *J. Rheol.* **34**, 553 (1990).
  - [3] M. D. Haw, W. C. K. Poon, and P. N. Pusey, *Phys. Rev. E* **57**, 6859 (1998).
  - [4] S. E. Paulin, B. J. Ackerson, and M. S. Wolfe, *Phys. Rev. E* **55**, 5812 (1997).
  - [5] J. Bender and N. J. Wagner, *J. Rheol.* **40**, 899 (1996).
  - [6] D. R. Foss and J. F. Brady, *J. Fluid Mech.* **407**, 167 (2000).
  - [7] J. F. Brady, *Curr. Opin. Colloid Interface Sci.* **1**, 472 (1996).
  - [8] T. G. Mason and D. A. Weitz, *Phys. Rev. Lett.* **75**, 2770 (1995).
  - [9] W. J. Frith, P. d'Haene, R. Buscall, and J. Mewis, *J. Rheol.* **40**, 531 (1996).
  - [10] H. Watanabe, M.-L. Yao, K. Osaki, T. Shikata, H. Niwa, and Y. Morishima, *Rheol. Acta* **38**, 2 (1999).
  - [11] B. J. Maranzano and N. J. Wagner, *J. Chem. Phys.* **114**, 10514 (2001).
  - [12] G. Bossis and J. F. Brady, *J. Chem. Phys.* **91**, 1866 (2000); D. R. Foss and J. F. Brady, *J. Rheol.* **44**, 629 (2000).
  - [13] J. R. Melrose, J. H. vanVliet, and R. C. Ball, *Phys. Rev. Lett.* **77**, 4660 (1996); R. S. Farr, J. R. Melrose, and R. C. Ball, *Phys. Rev. E* **55**, 7203 (1997).
  - [14] M. C. Newstein, H. Wang, N. P. Balsara, A. A. Lefebvre, Y. Shnidman, H. Watanabe, K. Osaki, T. Shikata, H. Niwa, and Y. Morishima, *J. Chem. Phys.* **111**, 4827 (1999).
  - [15] T. G. Mason, J. Bibette, and D. A. Weitz, *J. Colloid Interface Sci.* **179**, 439 (1996).
  - [16] P. Hébraud, F. Lequeux, J. P. Munch, and D. J. Pine, *Phys. Rev. Lett.* **78**, 4657 (1997).
  - [17] R. Höhler, S. Cohen-Addad, and H. Hoballah, *Phys. Rev. Lett.* **79**, 1154 (1997).
  - [18] P. Sollich, F. Lequeux, P. Hébraud, and M. E. Cates, *Phys. Rev. Lett.* **78**, 2020 (1997); P. Sollich, *Phys. Rev. E* **58**, 738 (1998).
  - [19] L. Berthier, J.-L. Barrat, and J. Kurchan, *Phys. Rev. E* **61**, 5464

- (2000); J.-L. Barrat and L. Berthier, *ibid.* **63**, 012503 (2000).
- [20] V. Breedveld, D. van den Ende, M. Bosscher, R. J. J. Jong-schaap, and J. Mellema, *Phys. Rev. E* **63**, 021403 (2001).
- [21] X. Qiu, H. D. Ou-Yang, D. J. Pine, and P. M. Chaikin, *Phys. Rev. Lett.* **61**, 2554 (1988).
- [22] J. F. Brady and J. Morris, *J. Fluid Mech.* **401**, 243 (1999).
- [23] W. van Meegen and P. N. Pusey, *Phys. Rev. A* **43**, 5429 (1991).
- [24] W. van Meegen and S. M. Underwood, *Phys. Rev. E* **49**, 4206 (1994).
- [25] J. B. Berne and R. Pecora, *Dynamic Light Scattering* (Wiley-Interscience Publications, New York, 1976).
- [26] G. Maret and P. E. Wolf, *Z. Phys.* **65**, 409 (1987).
- [27] D. J. Pine, D. A. Weitz, P. M. Chaikin, and E. Herbolzheimer, *Phys. Rev. Lett.* **60**, 1134 (1988).
- [28] D. A. Weitz and D. J. Pine, in *Dynamic Light Scattering, The Method and Some Applications*, edited by W. Brown (Oxford Science Publications, Oxford, 1993).
- [29] M. D. Haw, W. C. K. Poon, P. N. Pusey, P. H ebraud, and F. Lequeux, *Phys. Rev. E* **58**, 4673 (1998).
- [30] In view of these considerations we could, with the benefit of hindsight, have decided to work from the start in the single-scattering regime where the theory would have been unambiguous; we may investigate this possibility in future work. Note, however, that this would bring added experimental complications. For example, the samples would have to be “refractive-index-matched” using a mixture of two liquids; also, considerable care would be necessary to eliminate stray scattering from dust and the walls of the narrow-gap shear cell.
- [31] P. N. Pusey, in *Liquids, Freezing and the Glass Transition*, edited by J. P. Hansen, D. Levesque, and J. Zinn-Justin (Elsevier, Amsterdam, 1991).
- [32] P. N. Segr e and P. N. Pusey, *Phys. Rev. Lett.* **77**, 771 (1996).
- [33] C. M. Sorensen, R. C. Mockler, and W. J. O’Sullivan, *Phys. Rev. A* **14**, 1520 (1976).
- [34] P. N. Pusey, *J. Phys. (Paris)* **48**, 709 (1987).
- [35] P. Bartlett, *J. Chem. Phys.* **107**, 188 (1997).
- [36] W. Schaertl and H. Sillescu, *J. Stat. Phys.* **77**, 1007 (1994).
- [37] P. N. Segr e, W. van Meegen, P. N. Pusey, K. Sch atzel, and W. Peters, *J. Mod. Opt.* **42**, 1929 (1995).
- [38] G. Petekidis and P. N. Pusey (unpublished).
- [39] W. van Meegen, T. C. Mortensen, S. R. Williams, and J. M uller, *Phys. Rev. E* **58**, 6073 (1998).
- [40] J. P. Bouchaud, in *Soft and Fragile Matter, Nonequilibrium Dynamics, Metastability and Flow*, edited by M. E. Cates and M. R. Evans (Institute of Physics, London, 2000).
- [41] M. Cloitre, R. Borrega, and L. Leibler, *Phys. Rev. Lett.* **85**, 4819 (2000).
- [42] We are grateful to Daan Frenkel (private communication) for emphasizing the relevance of this observation to our experiments.
- [43] G. Petekidis, D. Vlassopoulos, and P. N. Pusey (unpublished).